NUMERICAL SIMULATIONS OF THE AERODYNAMIC LOAD DISTRIBUTIONS OVER THE VS-30 SOUNDING ROCKET

Diogo Mendes Pio, diogopio@gmail.com
Universidade do Vale do Paraíba – Univap, Av. Shishima Hifumi, 2911, São José dos Campos - SP
Edson Basso, basso@iae.cta.br
Instituto de Aeronáutica e Espaço, CTA/IAE/ALA, Pça. Mal. Eduardo Gomes, 50, São José dos Campos – SP
Carlos Eduardo de Souza, carloseduardos@iae.cta.br
Instituto de Aeronáutica e Espaço, CTA/IAE/ALA, Pça. Mal. Eduardo Gomes, 50, São José dos Campos – SP
João Luiz F. Azevedo, azevedo@iae.cta.br
Instituto de Aeronáutica e Espaço, CTA/IAE/ALA, Pça. Mal. Eduardo Gomes, 50, São José dos Campos – SP
Roberto Gil Annes da Silva, rasilva@iae.cta.br
Instituto de Aeronáutica e Espaço, CTA/IAE/ALA, Pça. Mal. Eduardo Gomes, 50, São José dos Campos – SP

Abstract. *This paper shows the initiative to use a code of Computational Fluid Dynamics (CFD) to calculate the properties of the flows over a sounding rocket configuration. The CFD code (Bru3d), developed at Institute of Aeronautics and Space (IAE) performs calculations based on Navier-Stokes, in a context of finite volume on unstructured meshes, with the use of turbulence modeling . The results are compared with those calculated by the software Missile Datcom as part of the process of verifying the CFD code. Graphs showing the distribution of axial and normal force, and the distribution of pressure coefficient (Cp) for various Mach numbers flow regimes. These results show that the CFD tool under development is able to predict the phenomena present in supersonic flows about sounding rocket configurations, and this code can be used to assist the phase of loads calculation on these vehicles.*

Keywords*: CFD; Sounding Rocket; Aerodynamics; Turbulent Flows*

1. INTRODUCTION

This article deals with the computational simulation of the VS-30 sounding rocket aerodynamics where the numerical calculation is performed by using the discretized Navier-Stokes equations. These equations are partial differential equations, nonlinear, assuming the fluid as a continuum. This formulation allows the calculation of compressible, viscous, turbulent flows, with the presence of discontinuities, thus forming a fairly complete tool for analyzing. Duarte (2007) used the Missile Datcom software to calculate pressure distribution over the VS-30 sounding rocket. It is intended that the results will be used to calculate the aerodynamic load distributed on the vehicle, together with the results of the Missile Datcom software, and the analysis and comparisons of these results is the emphasis of this work. Obtaining the numerical solution of any physical problem requires, first, the ability of creating the corresponding mathematical model. The mathematical model must be such that it can be solved by non-prohibitive computation times, and that the results adequately represent the physical phenomenon into account.

In this article will be present a comparative analysis of results obtained using the numerical code developed at the IAE (Bru3d) (Bigarella, 2007) to solve the Navier-Stokes equations discretized in a context of finite volume in three dimensions, and the current software used for the calculation of loads, Missile Datcom. The Missile Datcom is a widely used semi-empirical datasheet component build-up method for estimate the aerodynamic characteristics of stability and control of missiles (Blake, 1997).

In this paper, will be used flow with zero angle of attack because it was a previous comparative study, although both tools, Bru3d and Missile Datcom, can perform calculations with different angles of attack. Calculations with different angles of attack will be made later .

2. NUMERICAL METHOD

The numerical analysis of the problem can be divided into three phases, namely: computational mesh generation, numerical calculation itself of the flow properties across the computational domain, and analysis of results. Will be discussed in the next sections the most relevant aspects of the process of mesh generation and the formulation used in the numerical code used in this paper and the presentation of results and their comparisons with other available data. For this paper was used to probe geometry vehicle VS-30 V01. Figure 1 shows the main geometrical characteristics of the vehicle, which were used in defining the domain of calculation to the step of generating the computational meshes.

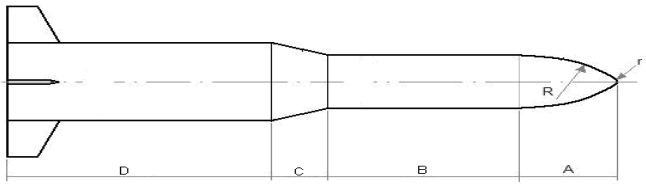

Figure 1. VS-30 V01 geometry details

For purposes of discussion of results the rocket will be divided into the following sections: Part A will be called cargo and Part B will be called the second stage, Part C will be called inter-stage, and Part D will be called the first stage. This configuration of the VS-30 have in part A two curves with different radii. It is important to note here that the simulated cases took into account the geometry of VS-30 without the fins, for further verification of these results in contrast with the calculation made by using DATCOM.

Computational mesh is, for the present work, the set of control volumes to discretize the domain of calculation around the vehicle. The mesh generation process begins by defining the appropriate values for the dimensions of control volumes in the different regions of the domain. For the control volumes near the surface of the vehicle, values for the maximum distances of the centroids of the volumes to the centroids of the faces of boundary are specified, taking into account the flow variables and turbulence model chosen. For example, in the case of flow with Mach number equal to 2, and the model Spalart-Allmaras turbulence, the thickness of first layer of control volumes near the surface is not higher than 0,001 m. After these definitions, generates a two-dimensional mesh on a plane of symmetry of the vehicle including the center line, which is then rotated around the axis of the vehicle to produce the final three-dimensional mesh for use in the simulations.

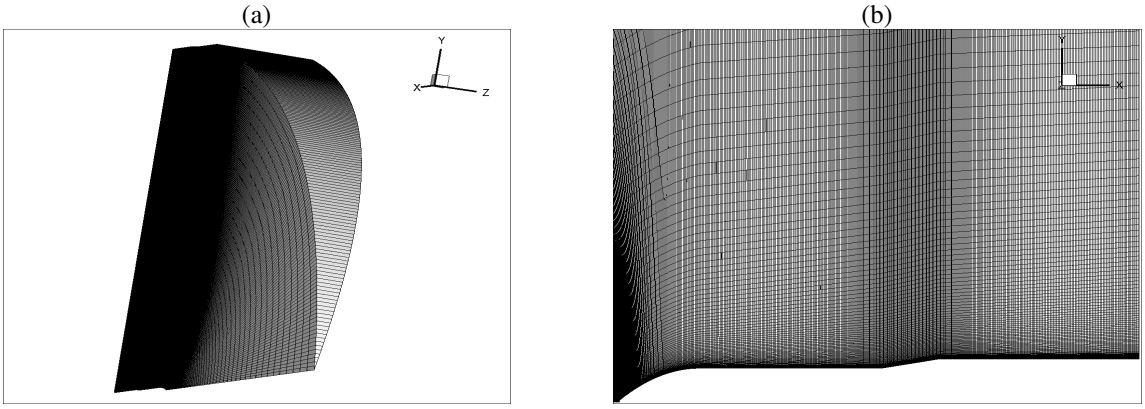

Figure 2. VS-30 computational grid.

It was carried out the numerical calculation of flow around the sounding rocket VS-30 in five different Mach numbers. They are: 1.1, 1.5, 2.0, 2.5 and 4.635. The properties of the flows below the Mach number of 4.635 are: density: 1.225 kg/m³; temperature: 288.15 K, pressure: 101 325 Pa. These Mach numbers were based on the properties of air at sea level. The simulation with Mach number equal to 4.635 has different properties, which were defined taking as basis the properties of air at 11km high. They are: density: 0.37468 Kg/m³; temperature: 218.1390 K; pressure: 23462.30 Pa. For each Mach number, the Reynolds number per meter associated was calculated, and these values are listed below:

Table 1. Values of Reynolds number per meter for each case studied.

Mach number	Reynolds number
1,1	25.076.628,35
1,5	34.195.402,30
2,0	45.593.869,73
2,5	56.992.337,16
4,635	35.689.563,73

The numerical code used in these calculations uses, for the discretization of spatial derivatives in the method, the Roe's scheme in finite volume, which has 2nd order accurate with the MUSCLE approach, in a context for unstructured

meshes. For the time marching process the code employs an implicit method associated with the use of convergence accelerators, such as multigrid and implicit residual smoothing. The code provides numerical values as a result of the density, of the components of velocity vector in the three directions of Cartesian axes, and the total energy. However, the semi-empirical Missile Datcom code used here, the code provides as a result the pressure coefficient (Cp), so that in order have a direct comparison, it was necessary to add some command lines in the code providing, then, a resulting Cp.

3. RESULTS

This section shows the qualitative result obtained with the simulation of Mach number of 1.1. The other simulations with higher Mach numbers possessed very similar results of properties field. Thus the figures will show only the results for this flow. In this simulation can be seen the emergence of a detached shock wave ahead of the VS-30. In Fig. 4a one can observe this shock wave just ahead of Part A. On the surface of the vehicle after the shock wave, one can perceive an increased flow velocity, which at the end of round (about 0.006 m) has a Mach number greater than 1.

Figure 4b is the detailed view of Fig. 4a, where the region of area A in the front of the vehicle was highlighted. It can be observed that the post-rounding region has an abrupt increase in the thickness of the boundary layer. This increase indicates a region of recirculating flow (most clear in the blue region). As the flow immediately before that recirculation is supersonic, may notice an appearance of a shock wave caused by the change of the geometry of the vehicle. Remember that this view is the result of a numeric simulation, there may be errors promoted by the turbulence model or by the mesh size chosen. Thus one cannot assert that the real flow has a recirculation. Due to what was observed in this result, a more detailed investigation, using other computational meshes and other turbulence models are currently being made. What further reinforces that this result is a product of the combination of mesh and the chosen turbulence model is that this region has a favorable pressure gradient, which helps to prevent detachment of the boundary layer. The recirculation region only occurred in the simulation of flow with Mach number 1.1 and 4.635.

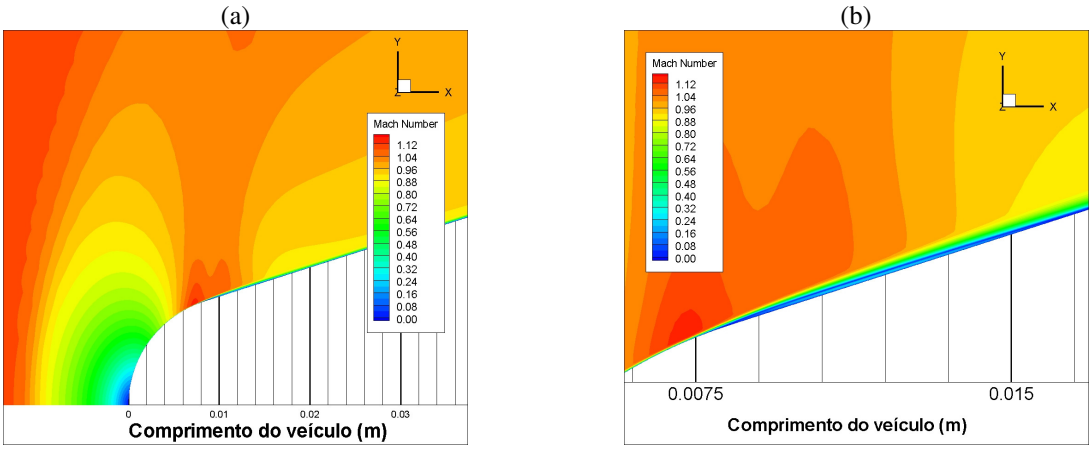

Figure 4. Flow over the payload compartment.

Figure 5a shows the result on the ramp from the rounding of the payload bay until the beginning of the cylindrical part of the second stage. It may be noted that this ramp promotes an acceleration of the flow where the Mach supersonic flow passes through the region in the payload bay. Figure 5b shows the flow region on the second stage. It can be observed that in this region there are only a thickening of the boundary layer, and this happens due to loss of energy by the flow. This energy has been dissipated due to the changing nature of energy, which passes from convective energy to energy of diffusion.

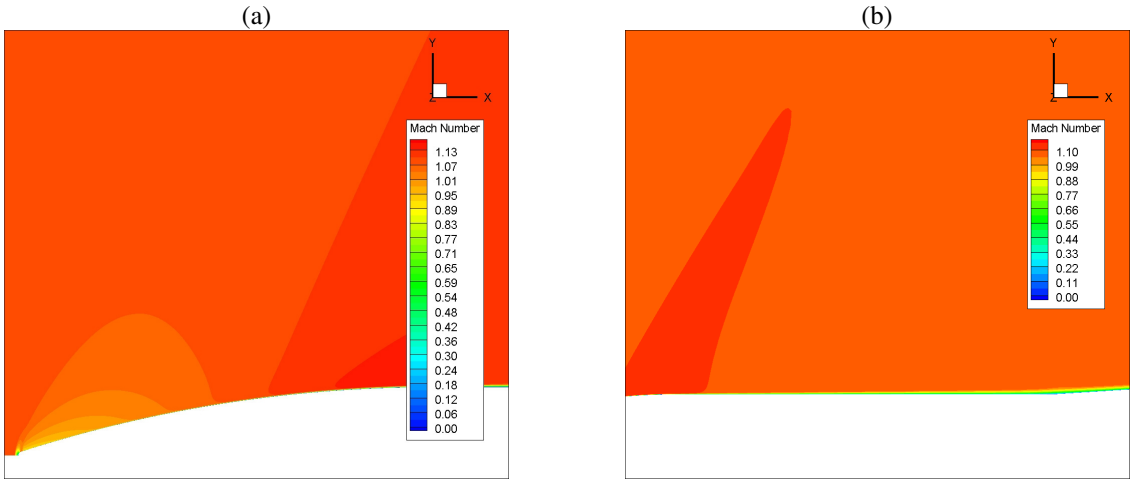

Figure 5. Flow over the payload compartment and over the second stage of the VS-30.

Figure 6 shows the flow in the region between the second stage and the inter-stage. This region has a slope in the geometry, which promotes the formation of a shock wave. However, in Fig. 5b was noted that the boundary layer thickens as it approaches this region, and this fact creates a smoother change of the flow causing the shock wave that forms is weak. This means that the flow has slowed, but did not become subsonic.

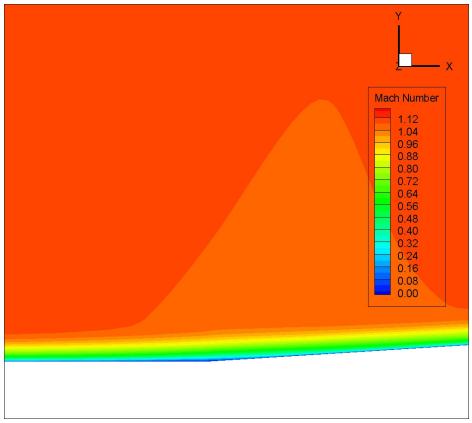

Figure 6. Flow over the second stage of the VS-30.

Figure 7a shows the region of the flow on the inter-stage. At the beginning of inter-stage one can observe the shock wave, the speed increase due to the slope and its end in a wave of expansion. In Fig. 7b one can be seen best in the region of the flow change angle geometry, with the onset of the expansion

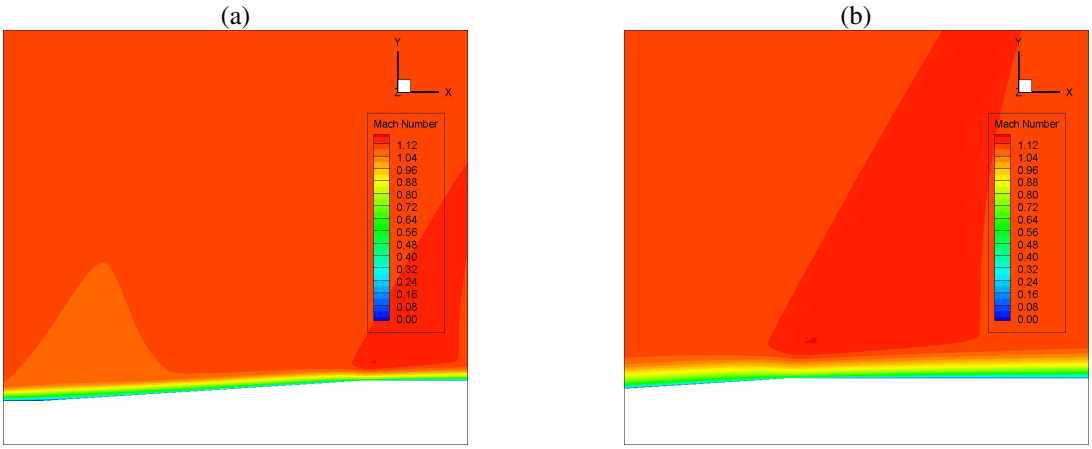

Figure 7. Flow at the inter-stage of the VS-30.

Figure 8 shows the flow over the first stage. It can be observed that the flow accelerates immediately after the inter-stage and then one can see the increase in the boundary layer, causing energy loss and increased shear force.

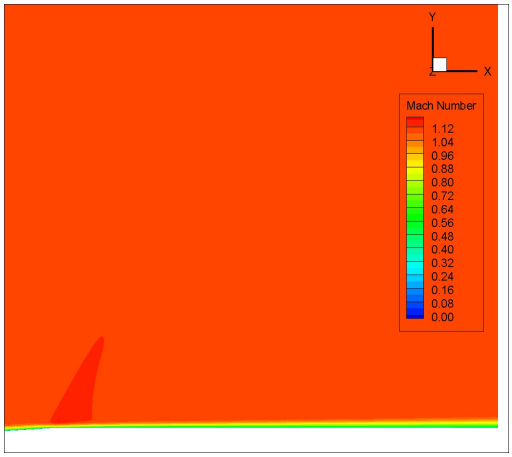

Figure 8. Flow over the first stage of the VS-30.

Figure 9 is a graph of axial force by meter due to pressure along the vehicle. It can be seen in the graph the quantitative details of the flow phenomena causing this distribution of force. The first detail to note is a peak axial force, or drag, on the edge of the vehicle. The second detail is the large increase in axial force in the region of the payload. As the regions B and D have a cylindrical geometry, the axial force is zero at these locations. It should be emphasized that there is no inclusion of the shear force in these results. Although the program has been implemented with the inclusion of viscous terms in the formulation, the results showed a strong predominance in determining the values of axial force due to normal pressure. In the inter-stage, again due to the change in geometry, there is a substantial increase in axial force. Immediately after this region, where the expansion occurs, the pressure dropped suddenly, returning almost to the value of the pressure of farfield flow.

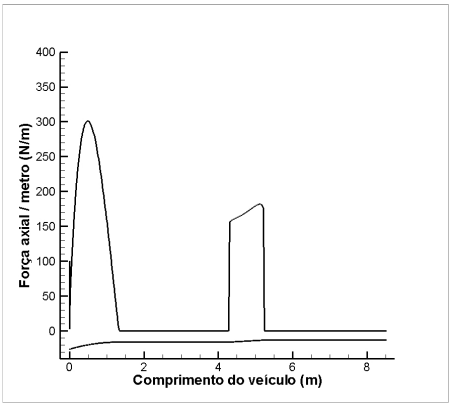

Figure 9. Graph of the axial force per meter vs. vehicle length.

In Fig.10 it is observed the graph of the normal force along the vehicle. This distribution is responsible for distribution of axial force seen in the previous figures, since the values of shear force were neglected. One can see that this normal force due to pressure has a maximum value in the region of the geometry, reducing its intensity before reaching the region B. For this figure it may be noted that the area of connection between the payload compartment and the second stage is subjected to a static pressure below that of the farfield flow. Another region on the surface of the vehicle subjected to large variations in pressure is the region of inter-stage. Through Fig. 10 can also notice a low pressure area immediately after this section on the first stage.

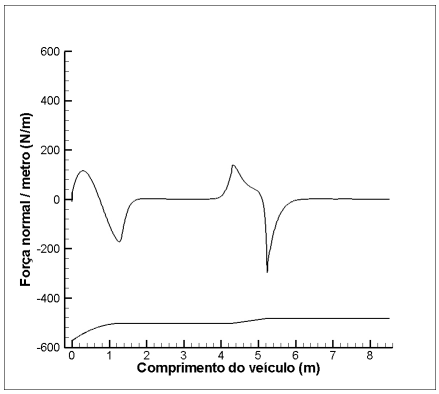

Figure 10. Graph of the normal force per meter vs. vehicle length.

The curve of pressure coefficient versus the length of the vehicle is shown in Fig. 11. This curve shows a behavior similar to the graphs of normal force, as expected. As Cp increases when there is an increase of pressure, one can see that there is an increase of Cp in front of the vehicle promoted by stagnation point in the flow. As noted in Fig. 4b, there is a recirculation flow in the region that causes a reduction in the amount of pressure. So there is a negative Cp in the region immediately following the end of the vehicle. The other aspects of the Cp curve follow the same trends already observed for the distribution curves of normal force. It is important noting that although the cylindrical regions of the first and second stages offer no geometrical variation can provide a value of Cp and axial force different from zero in these regions, the observed values are not totally zero. This is in line with expectations, since the flows were calculated using the Navier-Stokes equations, which permits the emergence of boundary layer, which change the way the flow perceive the presence of the geometry. As it is aerodynamic flow, and speeds are relatively high, these boundary layer are not very thick as to produce a very large effect on the values of axial force on the vehicle.

Also note that the graphs show large variations in the behavior of Cp. This occurs because the farfield flow having a Mach number close to the sonic regime, which leads the flow near the surface of the vehicle to more easily change their regime, and these effects generate large differences in pressure.

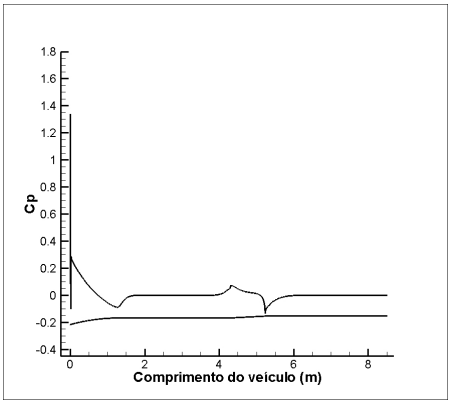

Figure 11. Graph of pressure coefficient (Cp) vs. vehicle length.

The following graphs are comparisons of the flows below the Mach number of 4.635. Note in Figs. 12a and 12b which, as the flow velocity increases, one can say that the maximum values in the graphs also increases almost linearly. In general, the curves for the distributions of normal force and axial force have very similar behaviors, which facilitates the prediction of the behavior of these property values for other speed regimes not simulated. Only in case the flow Mach number equal to 2.5 the curve of the normal force has a different behavior from others.

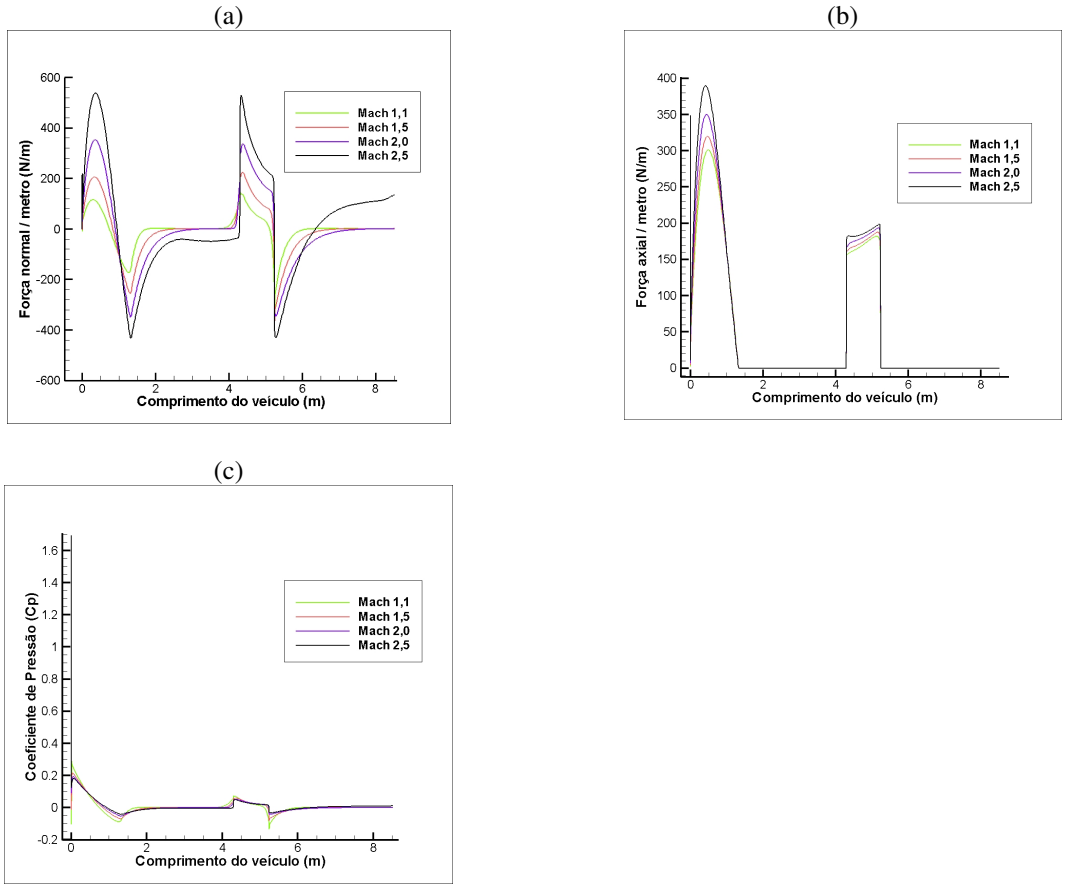

Figure 12. Distribution of normal force (a), Distribution of axial force (b), and Distribution of Cp (c) for the results at Mach numbers below 4.635.

For comparative purposes, and as an early form of verification of numerical results, there were simulations of flows in the software Missile Datcom with Mach numbers 1.5, 2.0 and 2.5, using the same properties of the flows. With these results were generated two graphs for each case, for normal force and pressure coefficient. By analyzing Figs. 13, 14 and 15 can be seen that the results in Bru3d have curves with less abrupt changes that the results of Missile Datcom. In general, the values for these variables agreed well between the codes. The biggest differences are in regions where the flow presents strong gradients of properties. These differences can be perceived because the code Bru3d be

able to better predict the flow in the boundary layer, theoretically. An example can be seen in the area of inter-stage, where there is clearly a region of interaction between the shock and the boundary layer. In this region, because the software Missile Datcom work only with geometric variations on previously calculated data, this software produces a sharp change in the values of Cp. In contrast, the code Bru3d presents a region where the thickness of the boundary layer plays a role in decreasing the maximum values of Cp and distribute this variation by a space along the abrupt change of geometry. Therefore, it is believed that the results of the code Bru3d can be nearest to the values of the flight of the vehicle. Of course only an experimental result or flight data may confirm this hypothesis.

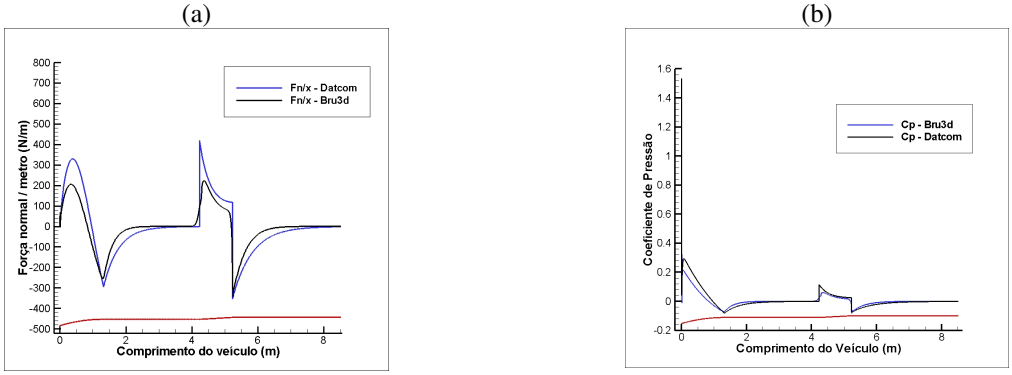

Figure 13 – Normal force distribution (a) and distribution of Cp (b) for Mach number 1.5.

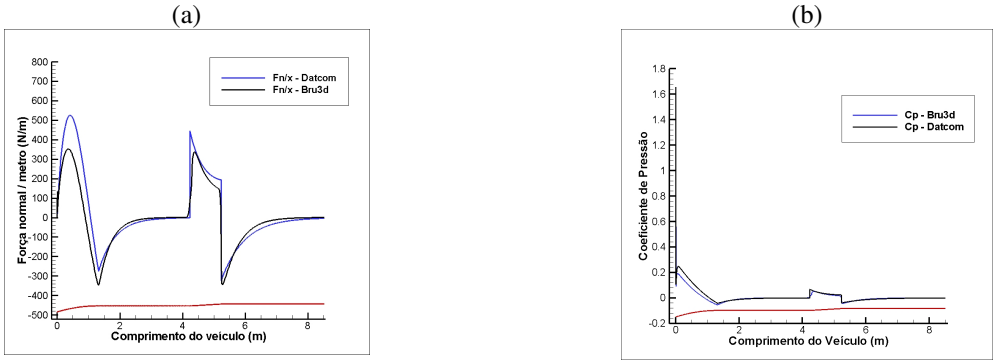

Figure 14 – Normal force distribution (a) and distribution of Cp (b) for Mach number 2.0.

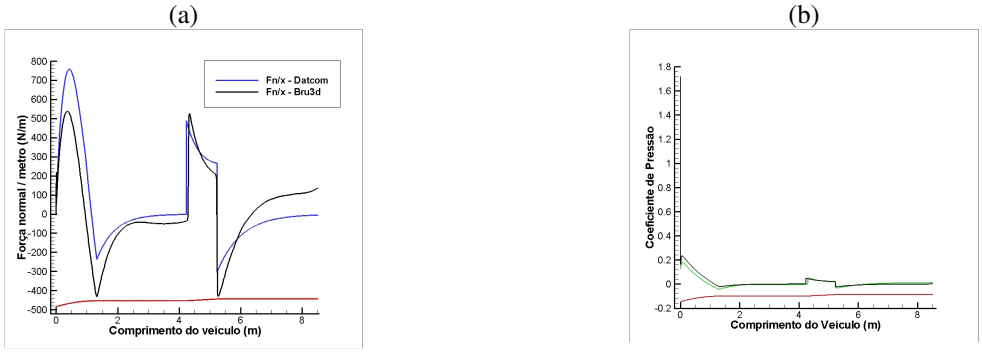

Figure 15 – Normal force distribution (a) and distribution of Cp (b) for Mach number 2.5.

So far the results have been shown and comparisons in the Mach numbers below 4.635. Will now analyze the case with Mach number of 4.635, where values of properties of the fluid was taken to an altitude of 11km. Figure 16a shows that the behavior of Cp both in Bru3d and in the Missile Datcom were very similar. Only at some points were observed degree of difference. The first region was on the edge of the vehicle shortly after rounding tip. Figure 16b shows this region and the difference in the values of Cp. Through this figure one can see that there is a tendency to detachment of the boundary layer just after the junction of the spherical tip of the vehicle with the tapered portion of the payload

bay. As mentioned earlier, this region has a favorable pressure gradient, not being a candidate region for the phenomenon of detachment, at first. For this reason, further tests are needed to eliminate the possibility of a result that still has influence of grid size, or even the turbulence model chosen. The second point is located in the inter-stage. Figure 16c shows that the difference between Bru3d and Missile Datcom can be described as previously, namely that as the Missile Datcom software that uses semi-empirical methods, differences in geometry generate sharp differences in the values of Cp, the contrary to the results observed in Bru3d code.

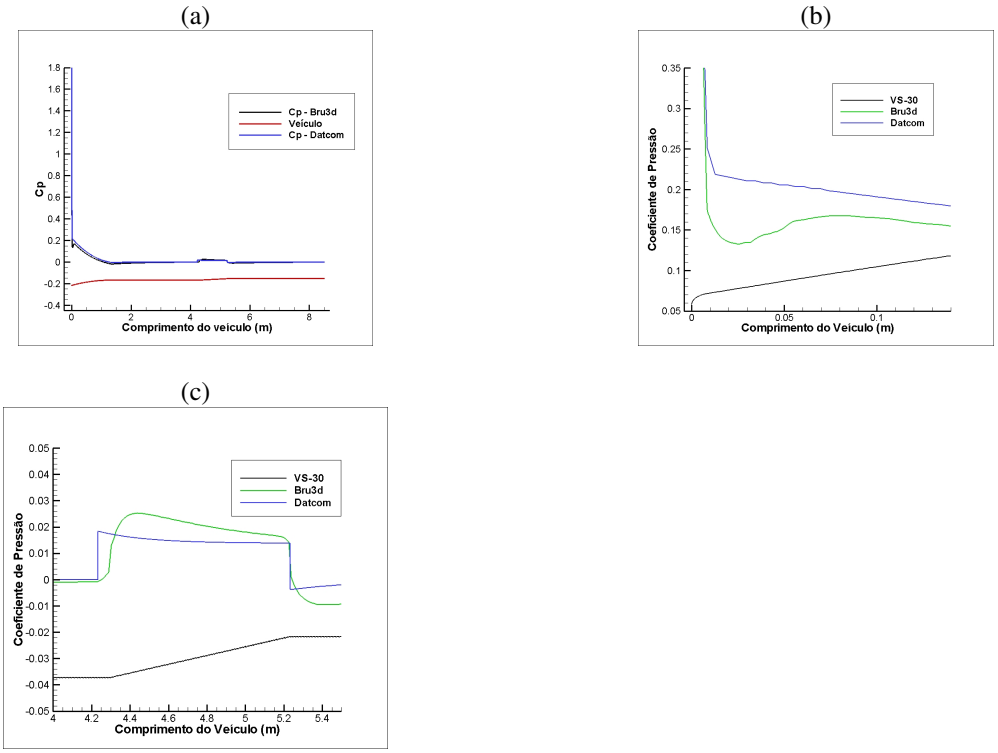

Figure 16 – Cp distribution for entire vehicle (a), over the tip of the vehicle (b), and over inter-stage (c).

4. CONCLUSIONS

Based on the results obtained in this work using a CFD tool for calculating the aerodynamics of the vehicle VS-30, and comparisons of these results with data obtained using the Missile Datcom, one can see that there are some differences between the values obtained with the two codes. The major differences coincide with regions of abrupt variation of the profile geometry. The regions where the geometry has a constant profile along the length of the vehicle, ie, regions where the diameter of the vehicle is constant for a certain range of coordinates in the direction of length, showed a reasonable agreement in results between the codes. In general, the Missile Datcom tends to focus more on the effects of these geometric variations, while the program Bru3d by its own nature, tends to calculate these geometric effects of variation in the flow surrounding them. Yet because of its formulation, the program Bru3d can bring more detailed information on the flows near the surface of the vehicle and support the complex phenomena that occur in a supersonic flow such as shock-boundary layer interactions.

5. REFERENCES

Duarte, G.F.R., 2007, “Análise de Sensibilidade de Cargas Aerodinâmicas em Relação à Variação de Parâmetros Geométricos em Veículos de Sondagem”, Trabalho de Graduação, Instituto Tecnológico de Aeronáutica, São José dos Campos, Brazil.

Bigarella, E.D.V., 2007, “Advanced turbulence modelling for complex aerospace applications”, Tese de Doutorado, Instituto Tecnológico de Aeronáutica, São José dos Campos, Brazil.

Blake, W.B., 1997, "Missile Datcom: 1997 Status and Future Plans". AIAA APPLIED AERODYNAMICS CONFERENCE. Atalanta, Estados Unidos.

6. RESPONSIBILITY NOTICE

The authors are the only responsible for the printed material included in this paper.